# In Search of New Physics at HERA

**Gerd W. Buschhorn**
**(H1 Collaboration)**

Max-Planck-Institut für Physik
(Werner-Heisenberg-Institut)
München

**Abstract.** An update is presented of the analysis of the H1 experiment at the HERA electron/positron-proton collider including the luminosity taken in 1997. Topics covered are: Status of the excess in deep-inelastic positron-proton scattering at very high $Q^2$ reported earlier and new results on neutral and charged current cross-sections at high $Q^2$, limits on the couplings of leptoquarks of the 1st and 3rd generation, limits on the production of excited fermions, observation of events with a high momentum isolated lepton and unbalanced transverse momentum. An outlook is given on the high luminosity upgrade of HERA and the H1 detector planned for 2000/2001.

## 1. Introduction

The HERA collider at the Deutsches Elektronensychrotron DESY in Hamburg went into operation in 1992. Electrons or positrons with an energy of 27.5 GeV are colliding with protons with an energy of 820 GeV yielding a center-of-mass energy of 300 GeV.

The unique features of HERA allow the investigation of the structure of the proton in kinematical regimes inaccessible so far. Fig. 1 shows how the two detectors H1 and ZEUS in the years 1994-1997 extended the range of $Q^2$ and $x$ in deep inelastic scattering beyond that of previous fixed target experiments.

In the first years of operation, the experiments concentrated on the small $x$ region where strong interaction properties of the proton were dominating. Meanwhile, the steady increase of the luminosity of HERA (Fig. 2)

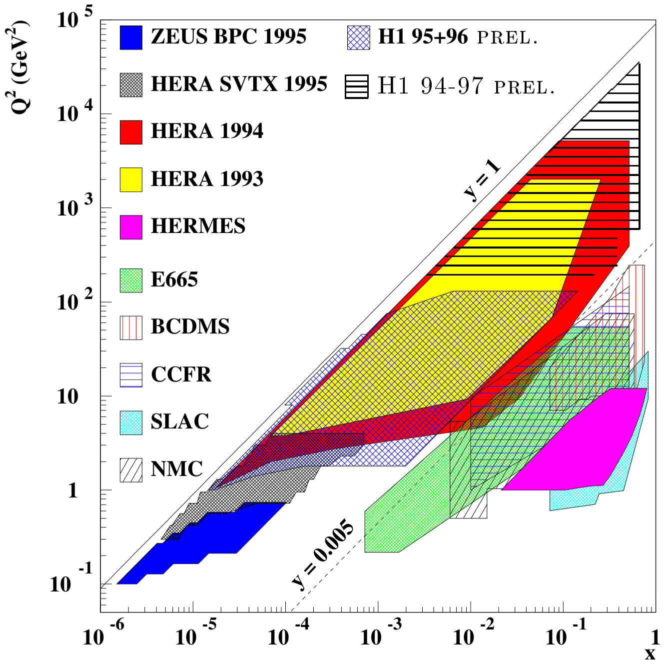


**Figure 1.** Regions in $x-Q^2$ covered by H1 and ZEUS in comparison with fixed target experiments.

also allows the study of weak interaction processes with increasing sensitivity.

In this paper, we present preliminary results from the H1 detector which include the full 1997 luminosity on deep-inelastic scattering (DIS) at high $Q^2$ (Chapter 2), limits on the couplings of leptoquarks (Chapter 3) and excited leptons (Chapter 4) and an update on events with an isolated high momentum lepton and unbalanced transverse momentum dubbed "odd lepton events" (Chapter 5). Some remarks on the planned upgrade of HERA and the H1 detector (Chapter 6) conclude the paper.

Details of HERA and the H1 detector can be found elsewhere [1], [2] and are not repeated here; the same holds for definitions and notations used in DIS [3].

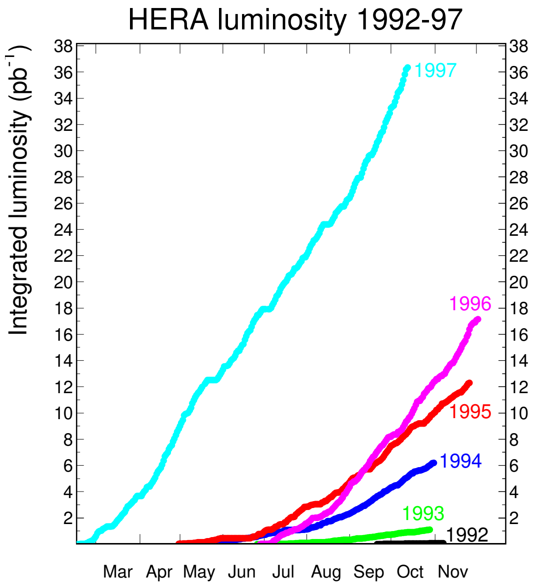


**Figure 2.** Yearly integrated luminosity of HERA running.

## 2. Deep inelastic scattering at high $Q^2$

### *2.1. The excess at very high* $Q^2$

In February 1997, H1 and ZEUS independently and simultaneously announced the observation of an excess of events compared with the standard model-expectation for DIS of positrons on protons at $Q^2 > 15.000$ GeV$^2$ [4], [5]. An update of the data with increased luminosity was presented in summer 1997 [6], [7]. The results gave rise to extended theoretical discussions on their interpretation in particular as leptoquarks produced as a s-channel lepton-quark resonance [8]. While the H1 data indicate some clustering of events at a lepton-quark mass of about 200 GeV, this is not supported by the combined analysis of H1 and ZEUS [9].

After summer 1997, both experiments further increased the collected luminosity; here we present the status of the H1 analysis including the full 1997 luminosity [10], [11]. For the analysis, the liquid argon calorimeter calibration has been improved *in situ* making use of the large NC event sample; it results in an electromagnetic energy resolu-

| $Q^2{}_{min}(\mathrm{GeV})^2$ | 2500 | 5000 | 10000 | 15000 | 20000 | 30000 |
|---|---|---|---|---|---|---|
| $N_{obs}$ | 1297 | 322 | 51 | 22 | 10 | 2 |
| $N_{DIS}$ | 1276 | 336 | 55 | 14.8 | 4.39 | 0.58 |
| | $\pm 98$ | $\pm 29.6$ | $\pm 6.4$ | $\pm 2.1$ | $\pm 0.73$ | $\pm 0.11$ |
| $P(N > N_{obs})$ | 42% | 56% | 60% | 5.9% | 1.8% | 11% |

**Table 1.** NC-events in the high $Q^2$-region: Observed ($N_{obs}$) and expected ($N_{DIS}$) number of events for $Q^2 > Q^2_{min}$ with the probability ($P$) for the observation of $N \geq N_{obs}$.

tion of $\sigma(E)/E_{em} = 12\%/\sqrt{E/GeV} \oplus 1\%$ with an error in the absolute energy calibration of $\Delta E/E_{em} = 1 - 3\%$ and a hadronic energy resolution $\sigma(E)/E_{had} = 50\%/\sqrt{E/GeV} \oplus 2\%$ with a corresponding error of $\Delta(E)/E_{had} = 4\%$; the error in the measurement of the electron angle amounts to $\Delta\Theta_e$=2-5 mrad.

While for neutral current (NC)-DIS events the scattered positron can be used in order to reconstruct the kinematic quantities $Q^2_e$, $y_e$ and $M_e = \sqrt{xs_ep}$ of each event, for charged current (CC)-events one has to rely on the less well measured hadrons for obtaining $Q^2_h$, $y_h$ and $M_h$. As has first been pointed out by Blondel and Jaquet [12], the hadronic quantity $\Sigma = \Sigma(E_h - P_{z,h})$, where $E_h$ and $P_{z,h}$ are the energy and longitudinal momentum component ($z$ = proton beam direction) of a hadron $h$ and the sum is taken over all measured hadrons, is less sensitive to hadrons which are produced in forward i.e. proton direction and escape detection by staying inside the beam pipe or are badly measured. For NC-events, a combination of leptonic and hadronic information was used in order to reduce errors resulting from the absolute energy calibration of the electromagnetic calorimeter or from initial state radiative losses of the lepton; for a detailed discussion see [4]. The analysis was performed taking into account the improved calorimeter calibration.

Including the 1997 runs, a total luminosity of 37 pb$^{-1}$ was collected by H1. Fig. 3 compares for NC events the measured $Q^2$-distribution with the standard DIS-Monte Carlo based on parton densities taken from the Martin-Roberts-Stirling MRSH parametrization and evolved to high $Q^2$ values using NLO-DGLAP equations (comp.[4]). Including the 1997 data results in a decrease of the significance of the previously reported excess, the 1997 data alone only marginally indicate an excess in the $Q^2 > 15.000$ GeV$^2$ region. The NC-results in the very high $Q^2$-region are summarized

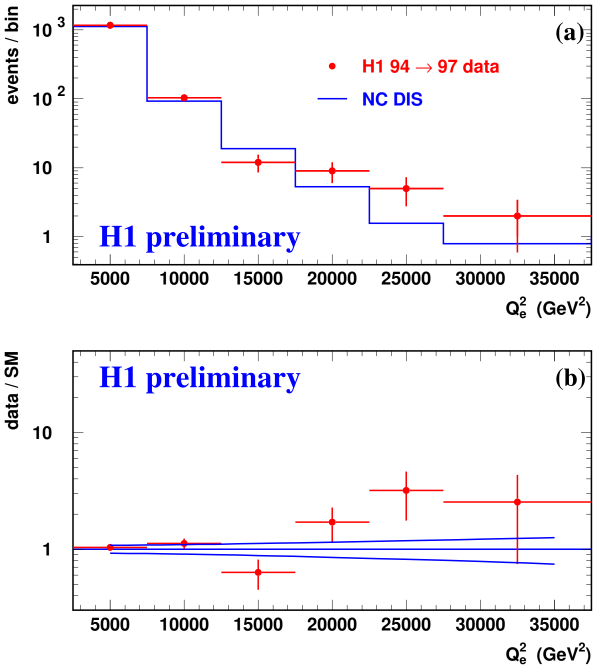


**Figure 3.** (a) $Q_e^2$ distribution of NC events (points) in comparison with standard DIS expectation (histogram). (b) Ratio of observed and expected number of NC events (points); the upper and lower line correspond to the $\pm$ $1\sigma$-error determined from combining statistical and systematic errors of the standard model expectation.

in Table 1.

The CC-results shown in Fig. 4 are summarized in Table 2. While a slight excess in the $Q^2 > 7.500$ GeV$^2$ region is observed, the data are compatible with the standard model within errors.

### *2.2. Inclusive high $Q^2$ NC/CC-cross sections*

The HERA data nevertheless immensely increase the knowledge of the DIS cross sections. A kinematic range of 200 GeV$^2$ $< Q^2 <$ 30.000 GeV$^2$ for $.005 < x < .65$ is covered by now enabling extended comparisons with QCD predictions.

The NC-differential cross section can be written as

| $Q^2{}_{min}(\mathrm{GeV})^2$ | 2500 | 7500 | 15000 |
|---|---|---|---|
| $N_{obs}$ | 100 | 41 | 9 |
| $N_{DIS}$ | 95.3<br>$\pm 16.7$ | 27.6<br>$\pm 8.4$ | 5.07<br>$\pm 2.8$ |
| $P(N > N_{obs})$ | 40% | 9% | 17% |

**Table 2.** CC-events in the high $Q^2$-region.

$$\frac{d^2\sigma^{NC}(e^{\pm}p)}{dxdQ^2} = \frac{2\pi\alpha^2}{xQ^4}\left[Y_+F_2(x,Q^2) - y^2F_L(x,Q^2) \mp Y_-xF_3(x,Q^2)\right] \quad (1)$$

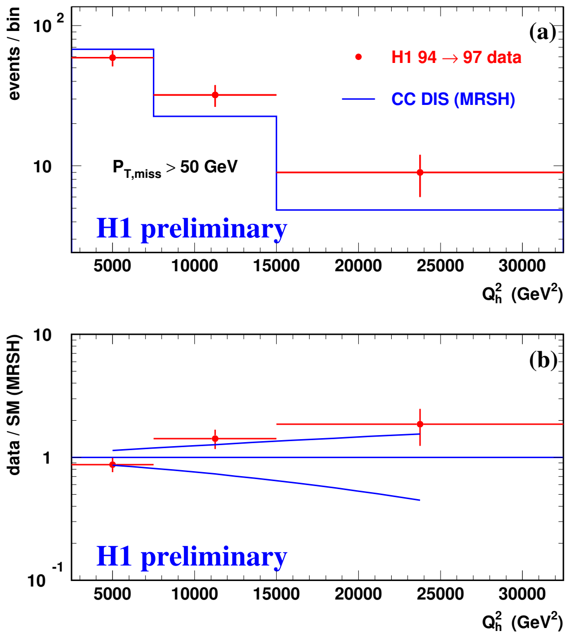


**Figure 4.** (a) $Q_h^2$ distribution of CC events. (b) Ratio of observed and expected number of CC events (for explanation see Fig. 3).

with the kinematical factors $Y_{\pm}(y) = 1 \pm (1-y)^2$ ($\pm$ for $e^{\pm}p$ - scattering). It can be approximated as

$$\frac{d^2\sigma^{NC}(e^{\pm}p)}{dxdQ^2} \cong \frac{2\pi\alpha^2}{xQ^4} Y_+ F_2(x,Q^2)$$

with corrections due to $F_3$ remaining $< 1\%$ for $Q^2 < 1.500$ GeV$^2$ and $< 10\%$ for $Q^2 = 5.000$ GeV$^2$ (at $x$=.08) and those due to $F_L$ being negligible for $y < .5$ and $\cong 5\%$ for $y = .9$, respectively. A "reduced cross section" is defined as

$$\sigma^{NC}(e^+p) = \frac{xQ^4}{2\pi\alpha^2}\frac{1}{Y_+}\frac{d^2\sigma}{dxdQ^2}. \tag{2}$$

In Fig. 5 the measured reduced cross section for $e^+p$-scattering in the high $x$-region is compared with the QCD prediction ([10], [11]). The MRSH prediction, based on measured parton densities, as well as the H1-NLO QCD fit which includes the new H1-high $Q^2$ data, describe the data well; in the high $x$- and high $Q^2$-region the H1 data are lowering the fit by up to 5%. The excess of the data observed in particular in the $x$= .45-distribution at the highest $Q^2$-values reflects the high $Q^2$-excess discussed in 2.1.

The CC-differential cross section may be written [3] in leading order QCD and neglecting quark mixing in terms of parton densities $xq(x,Q^2)$ as

$$\frac{d^2\sigma^{CC}(e^{\pm}p)}{dxdQ^2} = \frac{G_F^2}{2\pi}(P_W)^2\left[(\bar{u}+\bar{c}) + (1-y)^2(d+s)\right]$$

with the Fermi coupling constant $G_F = \pi\alpha/\sqrt{2}sin^2\Theta_W M_W^2$ and the $W$-propagator $P_W = M_W^2/(Q^2+M_W^2)$.

Similarly to (2), a reduced cross section is defined

$$\sigma^{CC}(e^+p) = \frac{2\pi x}{G_F^2}\left(\frac{Q^2+M_W^2}{M_W^2}\right)^2 \frac{d^2\sigma^{CC}}{dxdQ^2}$$

The measured $x$-integrated cross sections $d\sigma/dQ^2$ for NC- and CC-processes are compared in Fig. 6 with the standard model predictions. Good agreement within errors is found; the remaining difference between the two cross sections at high $Q^2$ is due to the different couplings of the neutral and charged current to the quark flavours as well as to the different propagators.

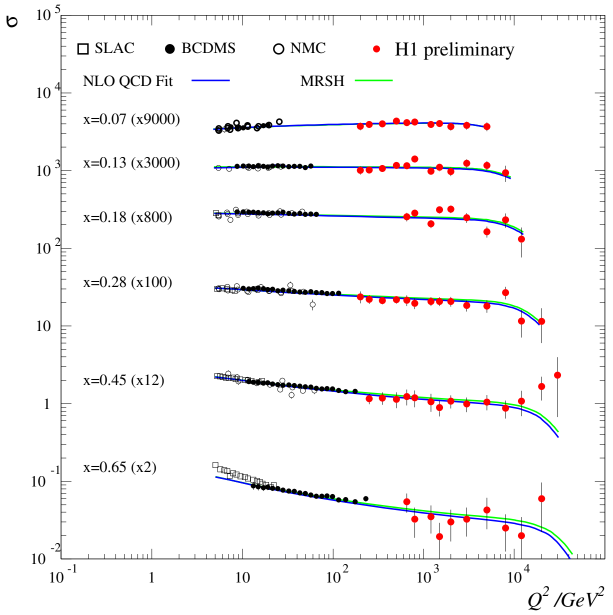


**Figure 5.** Reduced cross-section $\sigma^{NC}(e^+p)$ at fixed $x$ vs. $Q^2$ (1994-1997 data). The NLO QCD fit includes the H1 data.

## 3. Limits on leptoquark-production

The high $Q^2$-data can be used to derive limits on the couplings of leptoquarks (LQ). Preliminary results are presented for scalar LQ couplings to 1st and 3rd generation fermions for the 1994-1997 data corresponding to a total integrated luminosity of 37 pb$^{-1}$ [10], [11]. These results update the previous H1 analyses [14].

A scalar s-channel LQ is produced at a fixed mass $M = \sqrt{sx}$ with an intrinsic width $\Gamma = \lambda^2 M/16\pi$ where $\lambda$ is the dimensionless Yukawa coupling of the LQ to lepton-quark pair and a production cross section approximately given by [15] $\sigma = (\pi/4s)\lambda^2 q(x = M^2/s)$.

A LQ decaying into a 1st generation lepton and a quark jet cannot be distinguished from NC- or CC-DIS events on an event by event basis but statistically only by searching for a resonance peak in the invariant mass distribution and by making use of the decay angular distribution of the LQ. Scalar LQs decay isotropically in their CM-frame; with $y = (1 + cos\Theta^*)/2$ where $\Theta^*$ is the decay polar angle in the LQ CM frame, this results in a

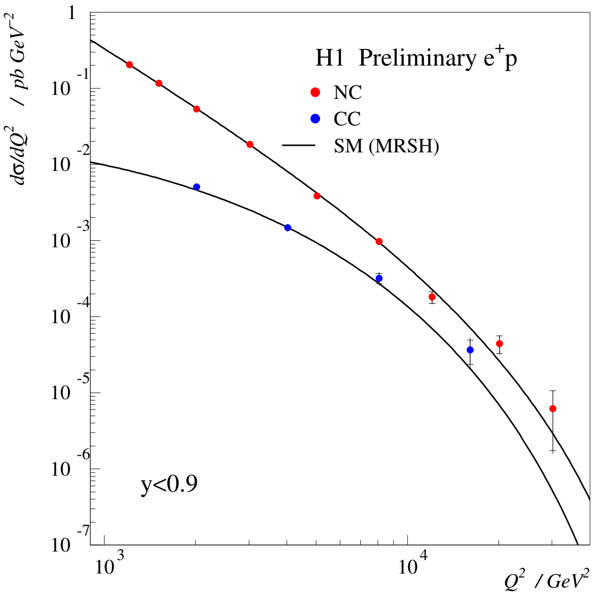


**Figure 6.** Differential cross-section $d^2\sigma/dxdQ^2$ for NC-events (upper data points) and CC-events (lower data points) in $e^+p$-scattering vs. $Q^2$ (1994-1997 data). Lines give the standard model prediction.

flat $d\sigma/dy$. In contrast, the dominating background from t-channel photon exchange at fixed $x$ is characterized by $d\sigma/dy \sim 1/y^2$. 1st generation LQs are, therefore, searched for in high mass NC- or CC-DIS events at high $y$. 2nd and 3rd generation LQs are characterized by an "exotic" final state i.e. the $\mu$ or $\tau$ and are, therefore, expected to be essentially free of background for high transverse momentum leptons. 2nd generation LQs are not further discussed here; the $\mu$-events discussed in Chapter 5 fail significantly the kinematic constraints for LQ production and no candidate for LQ$\rightarrow \mu$+jet was observed.

### *3.1. 1st generation LQs*

LQ$\rightarrow eq$: In order to maximize the significance of a LQ signal as a function of the LQ mass $M$, a mass dependent $y_e$-cut $y_{cut}(M)$ was applied such that only events with $y_e > y_{cut}(M)$ were accepted. The optimization of the cut was obtained from Monte Carlo studies; it ranges from $y_e \cong .5$ around $M_e$=45 GeV to $y_e \cong .1$ around $M_e$=250 GeV.

In Fig. 7a, the event distributions for NC-like candidates before and after applying the $y$-cut are compared with the expected distribution, taking into account the event detection efficiency. Details of this procedure and of the cut optimization are given in [15]. From the resulting limits on the LQ production cross section one can derive mass dependent limits on the coupling constant $\lambda$ keeping the branching ratio $\beta$ fixed e.g. due to a specific model or limits on $\beta$ keeping $\lambda$ fixed.

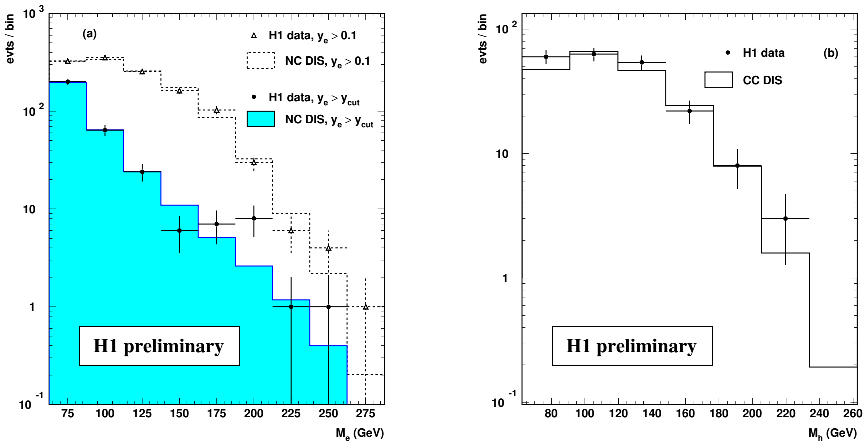


**Figure 7.** 1st generation on leptoquark analysis: (a) Mass distribution for NC DIS-like final states for different $y_e$-cuts i.e. $y_e > .1$ (fixed) and $y_e > y_{cut}$ (optimized). (b) Mass distribution for CC DIS-like final states with $P_T^{miss} >30$ GeV.

The limits obtained on $\lambda_{11}$ ($\lambda_{ij}$: $i$ = lepton generation, $j$= quark generation) shown in Fig. 8 are based on the LQ model of Buchmüller, Rückl and Wyler [16] in which for the 7 scalar LQs $\beta_e$ is fixed to .5 and 1, respectively. The new analysis improves earlier H1-results on LQs with fermionic number $F = 0$ [14] by about a factor of 3, implying $M_{LQ} > 275$ GeV (95% c.l.) for $\lambda^2/4\pi = \alpha_{em}$ i.e. $\lambda = 0.3$; for LQs with $F = 2$ the improvement is less significant. For this coupling strength the present LEP limit of 142 GeV [17] is not competitive with the new H1 limit.

The resulting constraints on $\beta_e$ for given $\lambda_{11}$ are shown in Fig. 9. A drop in sensitivity around $M = 210$ GeV is observed (note that $M_e$ underestimates $M_{LQ}$ by about 5 GeV). The H1-results extend the excluded domain beyond the $D0$ limits [18] in particular for u quark-couplings and small $\lambda$($\lambda = .1$ corresponds to $\alpha_{em}/10$).

<u>LQ$\rightarrow \nu q$</u>: Candidates for this channel correspond to CC-DIS events

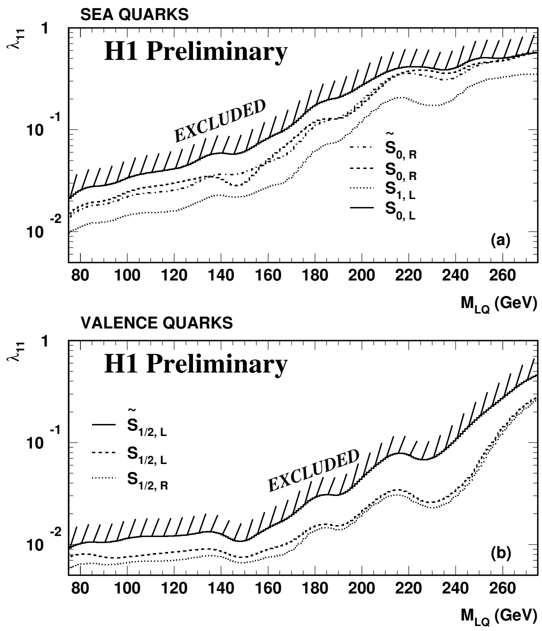


**Figure 8.** Exclusion limits (95% c.l.) on couplings $\lambda_{11}$ for scalar leptoquarks in the BRW-model: (a) fermionic number $F = 2$, (b) $F = 0$.

and, therefore, were searched for in an inclusive CC analysis with a cut of $P_T^{miss} > 30\text{GeV}$. The mass distribution shown in Fig. 7b is well described by the DIS-prediction.

Scalar LQs decaying to $eq$ with the branching ratio $\beta_e$ and to $\nu q$ with the branching ratio $\beta_\nu$ ($\beta_e + \beta_\nu \leq 1$) are outside the BRW model considered above. Gauge invariance implies that only the $e^+\bar{u}$-coupling contributes. The constraints on $\lambda_{11}$ are shown in Fig. 10. The combination of NC- and CC-DIS like channels results in an improvement of the $\lambda_{11}$ limit when compared with the pure NC-like channel ($\beta_e = 0.1$). For $\lambda = .3$ one finds $M_{LQ} > 210$ GeV (95%c.l.), far exceeding the TeVatron limit of $\cong 110$ GeV for such small $\beta_e$ [18], [19].

### *3.2. 3rd generation LQs*

LQs of this type with couplings $\lambda_{11}$ and $\lambda_{3j}$ are characterized by their decay into a jet and a $\tau$-lepton. The search was performed using the hadronic decay $\tau \rightarrow \text{hadrons} + \nu$, where the hadrons have the signature of a pencil like

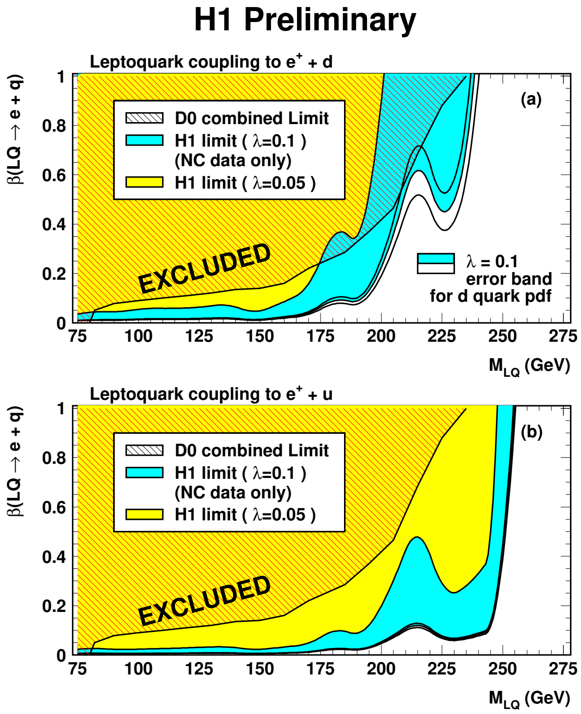


**Figure 9.** Limits on branching ratios $\beta_e$ of scalar leptoquarks formed in $e^+q$-fusion for fixed $\lambda$. (a) Leptoquark coupling to $e^+d$. For $\lambda = .1$ the $\pm 1\sigma$-error band due to uncertainties in the parton density functions is shown. (b) Leptoquark couplings to $e^+$u. Shown is also the $D0$ limit.

jet. Using simulated events the cuts in the mass distribution as well as in the multiplicity distribution of the jets were optimized. The event selection required 2 hadronic jets in the liquid argon calorimeter with $P_T > 30$ GeV where one jet has $\tau$-characteristics i.e. $M_{jet} < 7$ GeV and $1 \leq N_{tracks} \leq 3$.

Further cuts have been applied on the basis of Monte Carlo-studies of the $P_T^{miss}$- and $\Delta\phi$-distribution (with $\Delta\phi$ the azimuthal angle between the high multiplicity jet and the low multiplicity jet) of the LQ-decays. Setting the cuts to $P_T^{miss} > 10$ GeV and $\Delta\phi > 165^0$ leaves no event candidate where $.8 \pm .3$ events are expected.

Limits on $\lambda_{11}$ for a scalar LQ coupling to $e^+u$ for different branching ratios $\beta_e$, $\beta_\nu$ are derived as above and shown in Fig. 11a. For $\lambda_{11} = .3$ and $\beta_e = .1, \beta_\tau = .9$ a lower limit of $M > 275$ GeV (95% c.l.) is found; it is to be compared with the TeVatron limit of about 100 GeV obtained from $\tau\tau bb$- and $\nu\nu bb$- final states for $\beta_\tau = 1$ and $\beta_\nu$ =1 respectively [20], [21].

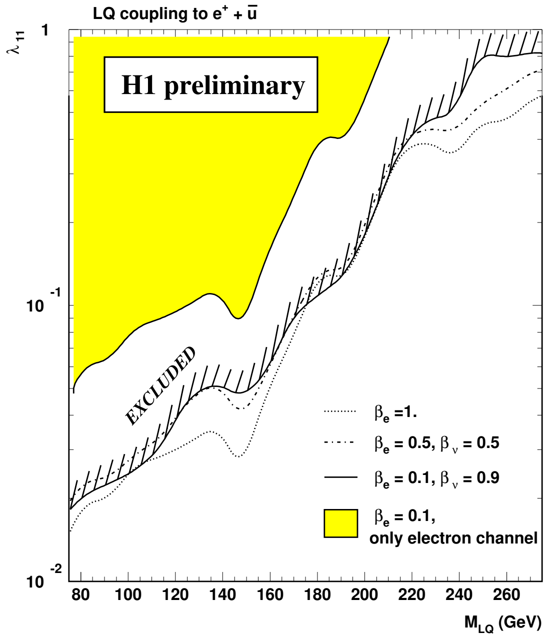


**Figure 10.** Limits on couplings $\lambda_{11}$ (95% c.l.) for scalar leptoquarks from $e^+p$-scattering for given $\beta_e$ and $\beta_\nu$.

Alternatively, limits on $\lambda_{3j}$ ($j = 1,2$) for different $\lambda_{11}$ assuming $\beta_e + \beta_\tau = 1$ are shown in Fig. 11b. For $\lambda_{11}$ and $\lambda_{3j}$ of electromagnetic strength, a limit of $M > 255$ GeV (95% c.l.) is obtained.

## 4. Excited Leptons

Excited leptons $e^*$ and $\nu^*$ decaying into a lepton and a gauge boson were searched for using the full 1994-1997 $ep$-luminosity of 37pb$^{-1}$ [13]. The results update and improve the previous H1 analysis [22].

For the 7 different final state topologies resulting from the 11 decay channels which have been considered the observed number of events is compared in Table 3 with the number predicted by the SM. The numbers of observed and expected events are compatible within errors and limits only on $\sigma \cdot \beta$ can be derived which improve the previous H1 results by about an order of magnitude.

In the specific model of Hagiwara, Komamiya and Zeppenfeld [23], the cross sections depend on coupling constants $f$ and $f'$ for the gauge groups SU(2) and U(1), respectively, as well as on a substructure scale $\Lambda$. Assuming specific relations between $f$ and $f'$, the branching ratios depend

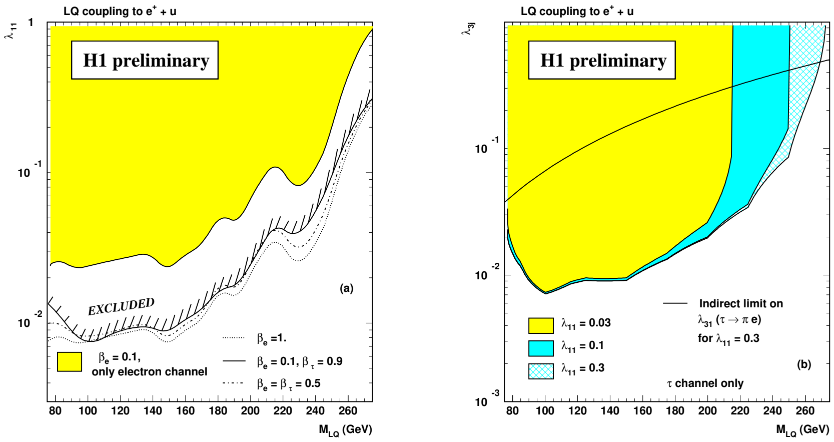


**Figure 11.** Exclusion limits (95% c.l.) on couplings $\lambda_{11}$ (a) and $\lambda_{3j}(j = 1.2)$ (b) for 3rd generation scalar leptoquarks from $e^+u$-fusion for different fixed $\beta_e$, $\beta_\tau$ and $\lambda_{11}$, respectively.

on $f/\Lambda$ and constraints on $f$ and $f'$ can be derived which are shown in Fig. 12. The LEP limits are more stringent but so far reach lower mass values only [24].

| Channel | Selection | Data | SM exp. | Efficiency |
|---|---|---|---|---|
| $e^* \to e\gamma$ | 2 EM clusters | 223 | 239 ± 7 | 85 % |
| $e^* \to eZ \hookrightarrow ee$ | 3 EM clusters | 3 | 1.4 ± 0.3 | 78 % |
| $e^* \to eZ \hookrightarrow \nu\bar{\nu}$ | 1 electron + $P_t^{miss}$ | 1 | 3.6 ± 0.7 | 70 % |
| $e^* \to eZ \hookrightarrow q\bar{q}$ | 2 jets + 1 electron | 38 | 48 ± 3 | 41 % |
| $e^* \to \nu W \hookrightarrow e\nu$ | 1 electron + $P_t^{miss}$ | 1 | 3.6 ± 0.7 | 70 % |
| $e^* \to \nu W \hookrightarrow q\bar{q}$ | 2 jets + $P_t^{miss}$ | 3 | 3.8 ± 0.5 | 40 % |
| $\nu^* \to \nu\gamma$ | 1 photon + $P_t^{miss}$ | 0 | 1.3 ± 0.8 | 38 % |
| $\nu^* \to \nu Z \hookrightarrow ee$ | 2 electrons + $P_t^{miss}$ | 0 | 0.38 ± 0.2 | 40 % |
| $\nu^* \to \nu Z \hookrightarrow q\bar{q}$ | 2 jets + $P_t^{miss}$ | 3 | 3.8 ± 0.5 | 40 % |
| $\nu^* \to eW \hookrightarrow e\nu$ | 2 electrons + $P_t^{miss}$ | 0 | 0.38 ± 0.2 | 40 % |
| $\nu^* \to eW \hookrightarrow q\bar{q}$ | 2 jets + 1 electron | 38 | 48 ± 3 | 41 % |

**Table 3.** Decay channels and final state topologies for excited leptons: Number of observed events vs. Standard Model expectation.

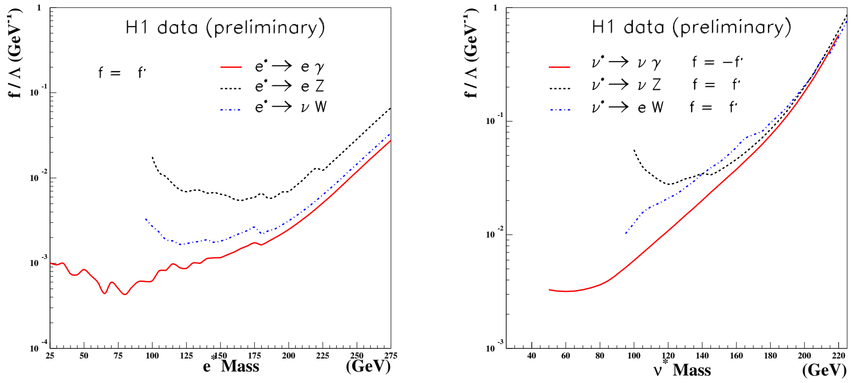


**Figure 12.** Exclusion limits (95% c.l.) for excited leptons as function of the lepton mass for $e^*$ (left) and $\nu^*$ (right).

## 5. "Odd leptons"

In 1994 with an integrated $e^+p$-luminosity of 3.2 pb$^{-1}$, an event was observed in the H1-detector [25] which showed an isolated high $P_T - \mu^+$ recoiling back to back in azimuth against a high $P_T$ hadronic system. The event is unbalanced in $P_T$ indicating an undetected particle in the final state. The event kinematics is compatible with $W$ production, the rate, however, is about a factor of 10 too high compared with the standard model-calculations of Baur, Vermaseren and Zeppenfeld [26] leaving room for other contributions. Here we present an update of the search for similar events based on the total $e^+p$-luminosity of 37 pb$^{-1}$ [27].

In order to identify events with significant missing transverse momentum, the standard H1-selection criteria for CC-DIS-events requiring in the calorimeter a $P_T > 25$ GeV have been applied. From the resulting event sample events with an isolated track were selected by essentially requiring a track with $P_T > 10$ GeV. In Fig. 13, the separation of these events to the closest hadronic jet ($D_{jet}$) as well as to the closest single particle track ($D_{track}$) is shown. The correlation between $D_{jet}$ and $D_{track}$ exhibits 6 events well separated from the rest (Fig. 13); applying in addition electron- and $\mu$-identification criteria shows that all the isolated tracks are due to leptons: $1e^-$, $2\mu^+$, $2\mu^-$, 1 $\mu$ of unidentified charge. Full details of the event kinematics are given in [27].

The imbalance in total transverse momentum $P_T^{miss}$ is ascribed to unobserved particles. Additional evidence for unobserved particles is provided by a significant deficit in longitudinal momentum balance in some

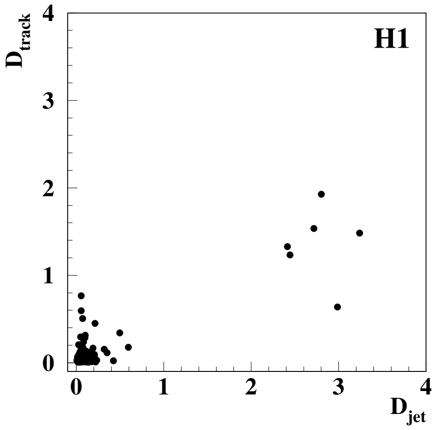


**Figure 13.** Correlation between the distances $D_{jet}$ and $D_{track}$ (see text) to the closest hadronic jet and closest track, respectively, for all high $P_T$ tracks in the inclusive event sample.

of the events and an acoplanarity $\Delta\phi$ between the high $P_T$-lepton and the hadronic system $X$ in most events. The correlation between $\Delta\phi$ and $P_T^{miss}$ for the six events is compared with that measured in standard NC events (subject to proper cuts in order to cover a similar kinematic region) in Fig. 14. Except for one $\mu^+$-event, the events are characterized by both high $\Delta\phi$ and high $P_T^{miss}$.

The rates for standard model processes which can yield lepton events of the observed type i.e. with an isolated high $P_T$ lepton and missing transverse momentum are summarized in Table 4. The $e^-$ event is compatible with the expected rate from $W$ production; the 5 $\mu$ events are to be compared with an expectation of .8 $\pm$ .2 events dominated by $W$ production and photon-photon-processes.

For the 6 events the kinematic parameters $P_T^X$ and $M_T^{\mu\nu}$ are compared in Fig. 15 with the distributions expected for $W$ production and photon-photon-processes (with $P_T^X$ = total hadronic transverse momentum of the event and $P_T^l$ = transverse momentum of the isolated lepton one has the high $P_T$ lepton-neutrino transverse mass $M_T^{l\nu} = \sqrt{(P_T^{miss} + P_T^l)^2 - (\vec{P}_T^{miss} + \vec{P}_T^{\nu})^2}$ where the measured missing transverse momentum $\vec{P}_T^{miss}$ is attributed to a neutrino). While the $e^-$ event and the $\mu 3$ event show kinematic properties typical for $W$ production and the $\mu 5$ event is compatible with $W$ production within $2\sigma$, the other $\mu$ events are found in regions of the phase space where the expected

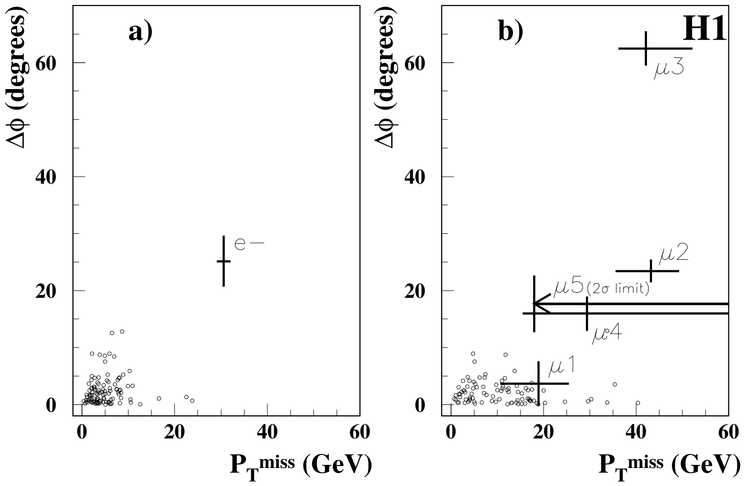


**Figure 14.** Distribution of events in the $P_T^{miss}$-$\Delta\phi$ plane. (a) electron channel: (b) muon channel. Crosses show the individual measurement errors, open circles show for comparison the NC event distribution (see text).

| | Electron Channel | Muon Channel |
|---|---|---|
| Data | $0\,e^+$, $1\,e^-$ | 5 |
| $W$ production | $1.65 \pm 0.47$ | $0.53 \pm 0.11$ |
| $Z$ production | $0.01 \pm 0.01$ | $0.01 \pm 0.01$ |
| CC - DIS | $0.02 \pm 0.01$ | $0.01 \pm 0.01$ |
| NC - DIS | $0.51 \pm 0.10\,e^+$, $0.02 \pm 0.01\,e^-$ | $0.09 \pm 0.06$ |
| Photoproduction | $< 0.02$ | $< 0.02$ |
| Heavy Quarks | $< 0.04$ | $< 0.04$ |
| Photon-Photon | $0.09 \pm 0.03\,e^+$, $0.04 \pm 0.01\,e^-$ | $0.14^{+0.14}_{-0.07}$ |

**Table 4.** Observed and predicted number of events with isolated high $P_T$-leptons$^{\pm}$ and $P_T^{miss}$.

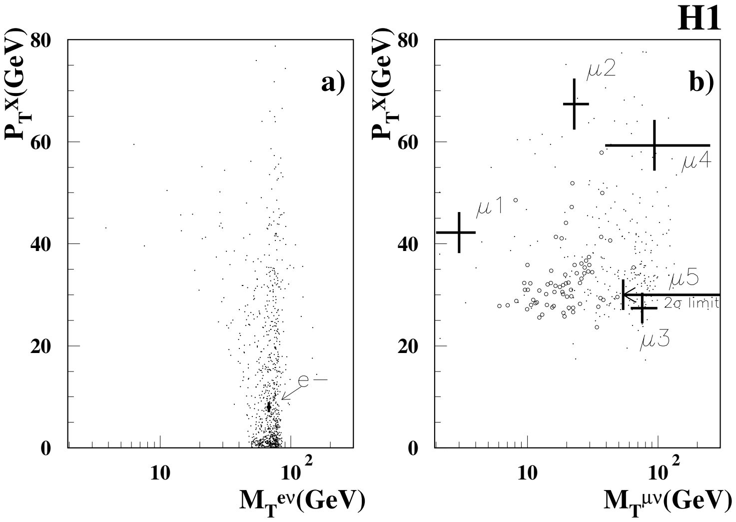


**Figure 15.** Distribution of events in $P_T^X$ and $M_T^{l\nu}$. (a) electron channel. (b) muon channel. Crosses indicate the $1\sigma$-uncertainty on the measured kinematical parameters of the observed events (for $\mu5$ the $2\sigma$-lower limit for $M_T^{l\nu}$ is shown). Expected events from an 500 x higher luminosity are shown for $W$ production (dots) and photon-photon-processes (open circles).

$W$ rate is low. $\mu2$ and $\mu4$ have a large $P_T^X$ and $\mu1$ has a small $M_T^{l\nu}$, both of which are unlikely for $W$ production or photon-photon-interaction. These three muon events are, therefore, unlikely to be due to the SM processes considered above.

## 6. Future Prospects

The scientific potential of HERA very much depends on the luminosity attainable. As the maximum possible beam currents have essentially been reached, a major increase of the luminosity can be achieved only by a modification of the beam optics. The standard approach is to reduce the beam cross section at the interaction point by reducing the $\beta$ function. The adopted solution which promises to lead to an increase of the luminosity at least by a factor of five foresees the installation of superconducting combined function magnets very close to the interaction point i.e. into the detectors. The luminosity increase is expected to become effective in the years 2000/2001.

The upgrade of the collider will be complemented by an upgrade of the H1 and ZEUS detector. In H1 besides improving the tracking components of the inner detector and increasing the sensivity of the liquid argon calorimeter, efforts are concentrating on improvement of the triggering including the development of advanced triggers.

A physically very interesting feature of HERA is the possibility to provide a longitudinal polarization of the $e^{\pm}$-beam. The polarized running mode of HERA foreseen after the luminosity upgrade obviously would profit from the higher luminosity and ensure a rich physics program for the first decade of the next century.

Acknowledgement: I am grateful to J. Meyer for his help and reading the manuscript.

## References

[1] G.-A. Voss, B.H. Wiik, Ann. Rev. Nucl. Part. Sci. **44** (1994) 413

[2] H1 Collab., I. Abt et. al., *Nucl. Instrum. Methods* **A. 386** (1997), 310, 348

[3] comp. e.g. A.M. Cooper-Sarkar, R.C.E. Devenish, A. DeRoeck, DESY 97-226

[4] H1 Collab., C. Adloff et. al., *Z. Phys.* **C74** (1997) 191

[5] ZEUS Collab., J. Breitweg et. al., *Z. Phys.* **C74** (1997) 207

[6] B. Straub, Int. Symp. on Lepton Photon Interactions, Hamburg 1997

[7] E. Elsen, Int. Europhys. Conf. on High Energy Physics, Jerusalem (1997)

[8] comp. e.g. G. Altarelli et. al., *Nucl. Phys.* **B506** (1997); G. Altarelli, CERN-TH. 97/278

[9] U. Bassler, G. Bernardi, DESY 97-136

[10] H1 Collab., Ph. Bruel, Rencontres de Moriond 1998

[11] H1 Collab., B. Heinemann, 6th Int. Workshop on Deep-Inelastic Scattering and QCD, Bruxelles (1998)

[12] A. Blondel, F. Jacquet, Proc. of the Study of an $ep$-Facility for Europe, ed. U. Amaldi, DESY 79-48

[13] H1 Collab., M.C. Cousinou, 6th Int. Workshop on Deep-Inelastic Scattering and QCD, Bruxelles (1998)

[14] H1 Collab., I. Abt et.al., *Nucl. Phys.* **B396** (1993) 3; ibid. T. Ahmed et.al., *Z. Phys.* **C64** (1994) 545; ibid. T. Ahmed et.al., *Phys. Lett.* **B369** (1996) 173

[15] B. Schrempp, Proc. Workshop Physics at HERA (1991), eds. W. Buchmüller and G. Ingelman, 1034

[16] W. Buchmüller, R. Rückl, D. Wyler, *Phys. Lett.* **B191** (1987) 442

[17] DELPHI Collab., F. Barao et.al., Contrib. to Int. Europhys. Conf. on High Energy Physics, Jerusalem (1997)

[18] $D0$ Collab., B. Abbott et.al., *Phys. Rev. Lett.* **79** (1997) 4321, **80** (1998) 2051

[19] CDF Collab., F. Abe et.al., *Phys. Rev. Lett.* **79** (1997) 4327

[20] CDF Collab., F. Abe et.al., *Phys. Rev. Lett.* **78** (1997) 2906

[21] $D0$ Collab., B. Abbott et.al., FERMILAB-PUB-98-081-E

[22] H1 Collab., T. Ahmed et.al., *Phys. Lett.* **B340** (1994) 205; H1 Collab., S. Aid et.al., *Nucl. Phys.* **B483** (1997) 44; see also ref.[14], I. Abt et.al.

[23] K. Hagiwara, S. Komamiya, D. Zeppenfeld, *Z. Phys.* **C29** (1985) 115

[24] DELPHI Collab., P. Abren et.al., *Phys. Lett.* **B393** (1997) 245; L3 Collab., M. Acciari et.al., *Phys. Lett.* **B401** (1997) 139

[25] H1 Collab., T. Ahmed et.al., DESY 94-248; H1 Collab., S. Aid et.al., *Z. Phys.* **C71** (1996) 211

[26] U. Bauer, J.A.M. Vermaseren, D. Zeppenfeld, *Nucl. Phys.* **B375** (1992) 3

[27] H1 Collab., C. Adloff et.al., DESY 98-063